Granular Matter (2022) 24:4
https://doi.org/10.1007/s10035-021-01147-w

ORIGINAL PAPER

A stress dilatancy relationship for coarse-grained soils incorporating particle breakage

Er-Lu Wu[1,2] · Jun-Gao Zhu[1,2] · Shun-Bin He[3] · Wen-Ming Peng[3]

Received: 12 June 2020 / Accepted: 21 July 2021 / Published online: 11 November 2021

Abstract
The energy consumption of particle breakage is added to the Cambridge energy balance equation so that the energy balance equation for coarse-grained soil is obtained. To reasonably measure the energy consumption of particle breakage, a function of friction coefficient relating to the axial strain is proposed to replace the friction coefficient as a constant in the energy balance equation based on the evolution rule of particle breakage. Then, according to the energy balance equation of coarse-grained soil, the energy consumption of particle breakage is calculated, and the particle breakage energy increases with axial strain increasing, which satisfies the thermodynamic law. Based on this energy balance equation, a simple stress dilatancy relationship is developed. In this stress dilatancy relationship, the relationship between $\mathrm{d}E_{\mathrm{b}}/p\mathrm{d}\varepsilon_{\mathrm{s}}$ and $M/\sqrt{M_{\mathrm{f}}}$ can be described by a simple function with acceptable accuracy. This stress dilatancy relationship is validated with the satisfactory capability to predict the dilatancy behavior of coarse-grained soils, which can be the effective choice to build the constitutive model.

Keywords Coarse-grained soil · Energy balance equation · Particle breakage · Particle breakage energy · Dilatancy

1 Introduction

Coarse-grained soil (CGS) has been widely used in earth–rockfill dams due to high shear strength and compaction capacity [1–4]. The accurate grasp of engineering properties of CGS is of significance to dam safety. It is well recognized that particle breakage can occur even at low stress levels [5–8], which greatly influenced the engineering behaviors of CGS [9–14], especially stress dilatancy behavior [15, 16]. The stress dilatancy relationship is significant for soil modelling. With incorporating the influence of particle breakage, the stress dilatancy relationship can make CGS modelling more accurately.

There are two most widely known stress–dilatancy relationships, Rowe's dilatancy theory [17] and dilatancy equation of Cambridge model [18]. Ueng and Chen modified Rowe's dilatancy theory with considering particle breakage energy, and derived a dilatancy law for CGS. However, according to Ueng and Chen's stress dilatancy relationship, the calculated value of particle breakage energy violates the thermodynamics law. Jia et al. [19], Mi et al. [20], and Guo and Zhu [21] all realized this contradiction and gave their own solutions. Then they developed their own dilatancy equations. Nevertheless, these dilatancy equations were complicated and the plastic potential function cannot be derived from the dilatancy equation. The stress dilatancy relationship of Cambridge model was simple and derived by assuming that the total input work was transformed into friction energy and elastic deformation energy of soil during triaxial shearing. Obviously, this assumed energy balance

✉ Jun-Gao Zhu
zhujungao@hhu.edu.cn

Er-Lu Wu
170804010004@hhu.edu.cn

Shun-Bin He
ylsdz@163.com

Wen-Ming Peng
pwm02@163.com

1 Key Laboratory of Ministry of Education for Geomechanics and Embankment Engineering, Hohai University, 01 Xikang Road, Nanjing 210098, China

2 Jiangsu Research Center of Geotechnical Engineering Technology, Hohai University, 01 Xikang Road, Nanjing 210098, China

3 China Power Construction Group Chengdu Survey and Design Institute Limited, 01 Huanhuabei Road, Chengdu, China

equation is suitable for clay. In order to obtain the energy balance equation for CGS, the particle breakage energy is added to this assumed energy balance equation in this paper. Then, according to this energy balance equation for CGS, a simple and practical stress dilatancy equation is developed incorporating the correction of friction coefficient based on the change law of particle breakage and the effect of the confining pressure on the critical state stress ratio.

2 Large-scale triaxial compression tests

CGS tested was obtained from Maji rockfill dam, China, and this tested material hereafter is called MRM. The particle shape is angular, and the maximum diameter of MRM is 60 mm. The particle size distribution (PSD) is shown in Fig. 1. The coefficient of uniformity C_u and the coefficient of curvature C_c are 6.00 and 1.50 respectively. MRM is classified as well-graded [22].

The large-scale triaxial testing apparatus in Hohai University is used in the tests, as seen in Fig. 2 [23]. This apparatus includes load cell, dial guage, triaxial cell, servo-control system, digital data collecting system, oil hydraulic system and water hydraulic system.

The large-scale triaxial compression test was carried out on MRM. The initial consolidated pressure, p_0, in the tests was 400, 800, 1600 and 2400 kPa, respectively. The initial dry density of the specimen was set as 2.2 g/cm^3. The specimen size was 300 mm in diameter by 600 mm in height. The soil of a specimen was divided into five equal parts, and compacted layer by layer into a cylinder. Each layer was compacted through a vibrator with a frequency of 70 cycles/s. The specimen was firstly subjected to the specific consolidated pressure. Then, it was sheared under a drained condition at a constant axial strain rate of 1 mm/min until the axial strain reached about 15%. Figure 3 shows the stress–strain–volume behaviors of MRM at different confining pressures.

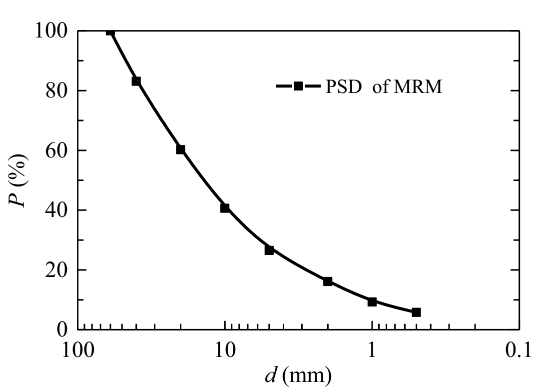

Fig. 1 Particle size distribution of MRM

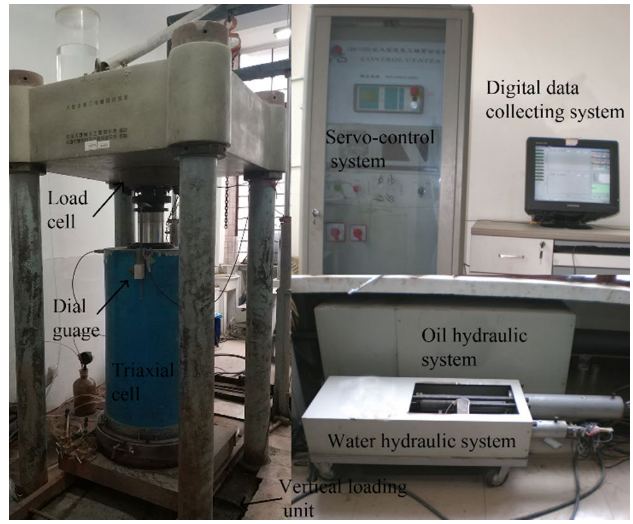

Fig. 2 The large-scale triaxial testing apparatus

3 Particle breakage energy

In the process of establishing Cambridge model for clay, Roscoe et al. [18] assumed that the sum of work done by the mean normal stress and the shear stress was the total

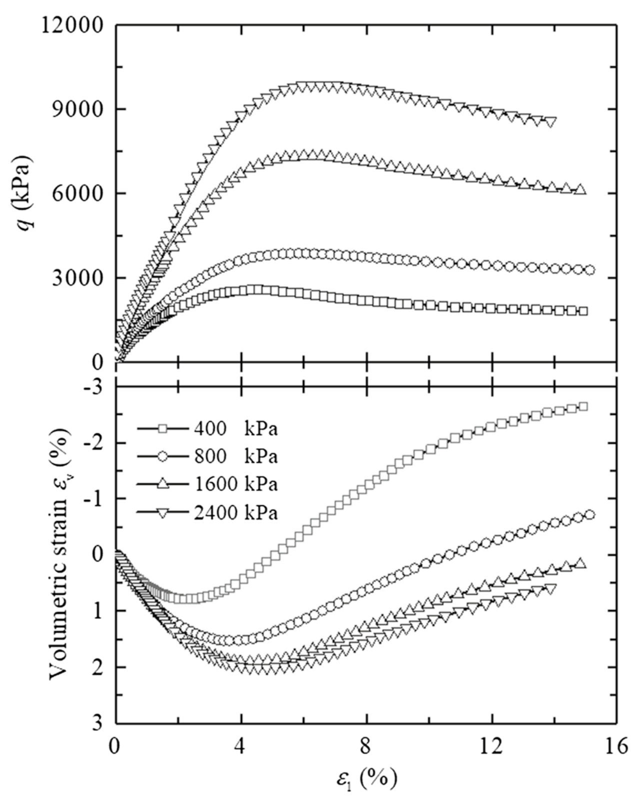

Fig. 3 Deviatoric stresses and volumetric strains against axial strain of MRM

input energy in the triaxial shear process, and the input energy was converted into the friction energy and elastic deformation energy. This energy balance equation for clay was expressed as

$$p\mathrm{d}\varepsilon_v + q\mathrm{d}\varepsilon_s = Mp\mathrm{d}\varepsilon_s + p\mathrm{d}\varepsilon_v^e \tag{1}$$

where $\mathrm{d}\varepsilon_v$ is the increment of volumetric strain, $\mathrm{d}\varepsilon_s$ is the increment of distortional strain, $\mathrm{d}\varepsilon_v^e$ is the increment of elastic volumetric strain, M is the friction coefficient and the value of M is the critical state stress ratio M_c, $p\mathrm{d}\varepsilon_v + q\mathrm{d}\varepsilon_s$ can be seen as the total work increment $\mathrm{d}E_t$, $Mp\mathrm{d}\varepsilon_s$ is the friction energy increment $\mathrm{d}E_f$, $p\mathrm{d}\varepsilon_v^e$ is the elastic deformation energy increment $\mathrm{d}E_e$.

Note that Eq. (1) was proposed for clay. Compared with clay, CGS has an obvious characteristic of particle breakage. Therefore, particle breakage energy should be considered in the energy balance equation for CGS. Thus, particle breakage energy is added into Eq. (1) to obtain the energy balance equation for CGS. That is

$$p\mathrm{d}\varepsilon_v + q\mathrm{d}\varepsilon_s = Mp\mathrm{d}\varepsilon_s + p\mathrm{d}\varepsilon_v^e + \mathrm{d}E_b \tag{2}$$

where $\mathrm{d}E_b$ is the particle breakage energy increment.

The increment of elastic volumetric strain can be ignored compared with the increment of total volumetric strain during triaxial shearing [24]. Therefore, Eq. (2) can be written as

$$p\mathrm{d}\varepsilon_v + q\mathrm{d}\varepsilon_s = Mp\mathrm{d}\varepsilon_s + \mathrm{d}E_b. \tag{3}$$

Notably, M_c needs to be confirmed before calculating $\mathrm{d}E_b$. The best method to obtain M_c is through the critical state of the test, but most times CGS tested cannot reach the critical state because of the restriction of test apparatus. Additionally, M_c has been found to be passively correlated with the confining pressures [25], which is like M_f. Therefore, the relationship between M_f and M_c is tried to find so that the value of M_c can be obtained easily based on M_f. For this purpose, coarse-grained soils for the large-scale triaxial tests all reached the critical state [26, 27], and the test data are arranged (Fig. 4). From the data in Fig. 4, it is apparent that the values of M_c/M_f all fall in the range of 0.8–1. For the sake of simplicity, the relationship between M_f and M_c is suggested as

$$M_c = 0.9M_f \tag{4}$$

where M_f is the peak stress ratio, which can be determined directly in the triaxial shearing test.

The values of M_f can be determined from the data in Fig. 3. Then, M_c can be obtained according to Eq. (4) and particle breakage energy is calculated based on Eq. (3), as shown in Fig. 5.

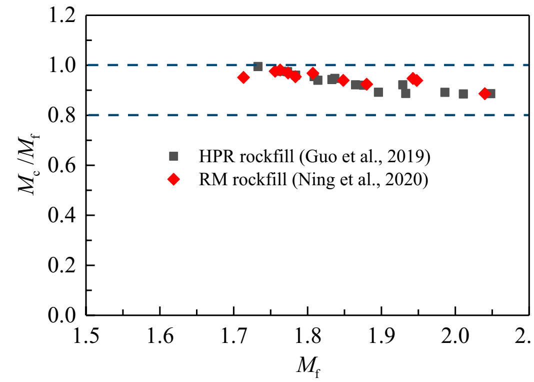

Fig. 4 Relationship between M_f and M_c

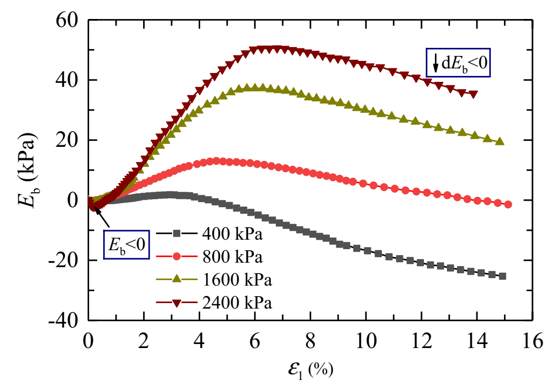

Fig. 5 Particle breakage energy of MRM ($M = M_c$)

Particle breakage is essentially a process of energy conversion. Notably the particle breakage is the unidirectional process, the energy consumption by particle breakage is also the unidirectional process. However, as indicated in Fig. 5, the value of E_b under each confining pressure is not only negative in the initial stage of the test but also appearing decreasing in the loading of the test, which violate the unidirectional process and the thermodynamics law. As can be seen from Eq. (3), the measurement of E_b depends on p, q, $\mathrm{d}\varepsilon_v$, $\mathrm{d}\varepsilon_s$ and M_c, and the values of p, q, $\mathrm{d}\varepsilon_v$, and $\mathrm{d}\varepsilon_s$ can be obtained directly in the triaxial test. That is to say, the assumption of Cambridge energy balance equation that taking the value of M as M_c makes the calculated friction energy larger so that the calculated particle breakage energy breaks the unidirectional process. Therefore, the friction coefficient of Eq. (3) needs to be modified to follow the unidirectional process so that reasonable calculation of particle breakage energy is realized.

As mentioned previously, particle breakage is a process energy conversion in essence. Then, the research on the particle breakage energy should be based on the research on the evolution law of particle breakage. That is, the calculation of particle breakage energy should be related to the evolution law of particle breakage. Beyond that, the reasonable calculation of particle breakage energy depends on the value of the friction coefficient. Hence the determination of M should be combined with the evolution law of particle breakage.

To investigated the evolution law of particle breakage under the whole shear process, the particle breakage data [28, 29] was rearranged, as seen in Table 1. The experimental evidence indicates that the relationship between the particle breakage index B_E [30], the confining pressure and the axial strain can be expressed as

$$B_E = \alpha \arctan\left(\lambda \varepsilon_1\right)\left(\sigma_3/p_a\right)^c \tag{5}$$

where α, λ and c are three material constants.

The test data of the particle breakage index B_E, the confining pressure and the axial strain were fitted by Eq. (5), as seen in Fig. 6. Apparently, Fig. 6 demonstrates that the fitting data are close to the experimental data. Therefore,

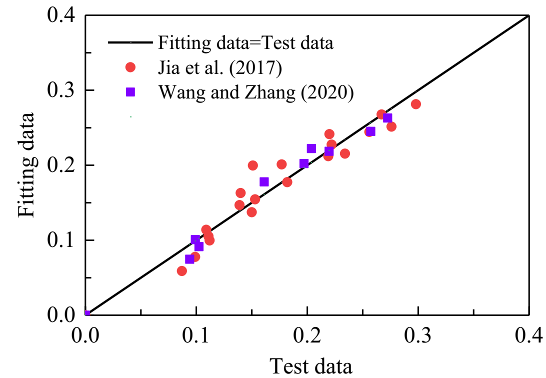

Fig. 6 Measured data and fitting data of particle breakage index

the evolution law of particle breakage under the whole shear process can be described by Eq. (5).

Notably, there are small relative motions between particles in the initial stage of the experiment. Thus, the friction coefficient is small, so is the particle breakage value. During the test, the soil deformation gets aggravating, and soil particles appear weltering and rearranging. Consequently, the friction coefficient increases all the time, so is the particle breakage value. When the soil reaches the critical state, the particle breakage value tends to be constant, and the energy consumption of particle breakage remains unchanged. That is, $dE_b = 0$. Additionally, $d\varepsilon_v = 0$ and $q/p = M_c$ at the critical state. Substituting the three values into Eq. (3), and rearranging, it can be obtained that $M = M_c$. Generally, the function of the friction coefficient should satisfy these conditions that it has a small value in the initial stage, increases with the axial strain increasing, and is equal to M_c at the critical state.

Based on the above analysis, the variation of the friction coefficient is similar to the change law of particle breakage value against the axial strain. Noting that the confining pressure is constant under the test, hence the formula of M neglects the influence of the confining pressure, and is proposed as

$$\frac{M}{M_c} = \alpha \arctan(\lambda \varepsilon_1). \tag{6}$$

Given that the friction coefficient should satisfy these conditions that it has a small value in the initial stage, increases with the axial strain increasing, and is equal to M_c at the critical state. When ε_1 goes to infinity, the value of M is M_c. Substituting this condition into Eq. (6), α can be obtained as $2/\pi$. Additionally, λ can be estimated as $\lambda = 12.7/\varepsilon_{1c}$ and ε_{1c} is the axial strain when the soil reaches the critical state. It is apparent from Eq. (11) that when the soil reaches the critical state, M/M_c cannot be equal to 1 from the mathematical point of view. Hence, when the value of M/M_c reaches 0.95, it can be considered that the

Table 1 Particle breakage data of coarse-grained soils

References	σ_3 (kPa)	ε_1 (%)	B_E (%)
Jia et al. [28]	500	2.15	8.7
	500	4.72	11.1
	500	8.20	15.0
	500	11.2	15.3
	500	15.1	14.0
	1000	2.16	9.90
	1000	5.24	13.9
	1000	7.85	18.2
	1000	11.2	15.1
	1000	15.5	23.4
	1500	2.40	22.1
	1500	8.24	21.9
	1500	10.1	22.2
	1500	13.3	25.6
	1500	15.2	27.6
	2000	2.46	10.9
	2000	5.66	17.7
	2000	8.62	22.0
	2000	12.1	26.7
	2000	15.1	29.8
Wang et al. [29]	1000	2.16	9.4
	1000	7.84	16.1
	1000	15.1	22.0
	1500	2.41	10.2
	1500	8.24	19.7
	1500	15.6	25.7
	2000	2.47	9.91
	2000	8.61	20.4
	2000	15.1	27.2

soil reaches the critical state. That is, $\frac{2}{\pi}\arctan(\lambda\varepsilon_s) = 0.95$ is seen as the sign of the soil reaching critical state, and $\lambda = 12.7/\varepsilon_{1c}$. Therefore, Eq. (6) can be rewritten as

$$M = \frac{2}{\pi}M_c \arctan(\lambda\varepsilon_1). \tag{7}$$

With Eqs. (3), (4) and (7), particle breakage energy can be calculated. Noting that p, q, $d\varepsilon_v$, $d\varepsilon_s$ and M_c can be obtained in triaxial test. Taking ε_{1c} as 40%, correspondingly λ is 31.8, and the reason for this will be discussed next. Then particle breakage energy of MRM is calculated again, as illustrated in Fig. 7. As expected, E_b increases with ε_1 increasing and tend to be stable, which follows the irreversible law of particle breakage. Therefore, the reasonable calculation of particle breakage energy is realized with Eq. (3) incorporating the correction of friction coefficient and the effect of the confining pressure on the critical state stress ratio.

4 Stress dilatancy relationship

Given that $d\varepsilon_v^p / d\varepsilon_s^p$ can be regard as equal to $d\varepsilon_v / d\varepsilon_s$ [24], to obtain the stress dilatancy relationship, Eq. (3) can be rewritten as

$$d_g = \frac{d\varepsilon_v^p}{d\varepsilon_s^p} = \frac{d\varepsilon_v}{d\varepsilon_s} = M - \eta + \frac{dE_b}{p d\varepsilon_s}. \tag{8}$$

Especially, the determination of $\frac{dE_b}{p d\varepsilon_s}$ is much cumbersome. If it can be replaced by one simple mathematical expression in terms of other variants, the stress dilatancy relationship, Eq. (8), can be better used conveniently. For this reason, the value of $\frac{dE_b}{p d\varepsilon_s}$ is calculated. The computed $\frac{dE_b}{p d\varepsilon_s}$ values are then plotted against $M / \sqrt{M_f}$ values (Fig. 8). As Fig. 8 shows, there is a simple relationship between $\frac{dE_b}{p d\varepsilon_s}$ and $M / \sqrt{M_f}$, as given by

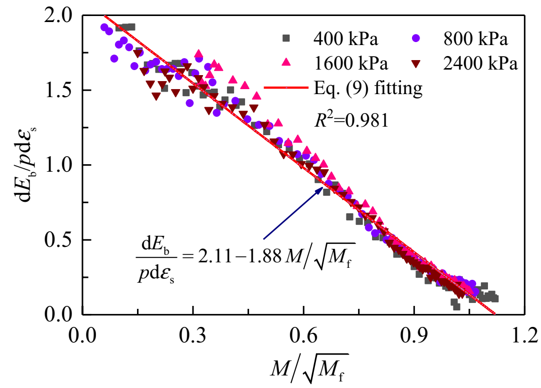

Fig. 8 Relationship between $\frac{dE_b}{p d\varepsilon_s}$ and $M / \sqrt{M_f}$ of MRM

$$\frac{dE_b}{p d\varepsilon_s} = A + BM / \sqrt{M_f} \tag{9}$$

where A and B are the material constants.

Figure 8 indicates Eq. (9) can describe the relationship between $\frac{dE_b}{p d\varepsilon_s}$ and $M / \sqrt{M_f}$ well. Substitution of Eq. (9) into Eq. (8) gives

$$d_g = M - \eta + A + BM / \sqrt{M_f}. \tag{10}$$

Cambridge dilatancy relationship can be given as

$$d_g = M_c - \eta. \tag{11}$$

Predictions of Eq. (10) and Cambridge law [Eq. (11)] on the dilatancy behavior of MRM are plotted in Fig. 9. As presented in Fig. 9, the confining pressure affects the dilatancy behavior of coarse-grained soils. However, the curves expressed by Cambridge law under various confining pressures are the same. That is, Cambridge law cannot well predict the dilatancy behavior under different confining pressures. By contrast, the proposed dilatancy equation [Eq.

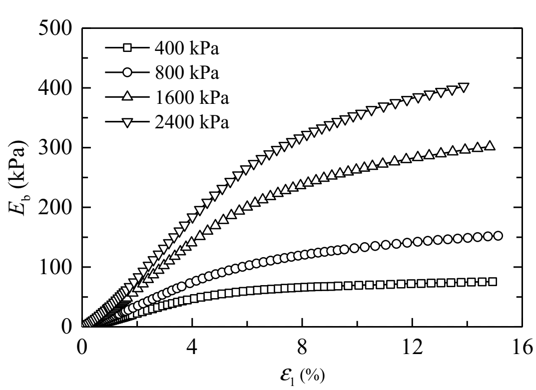

Fig. 7 Energy consumption of particle breakage (variable M)

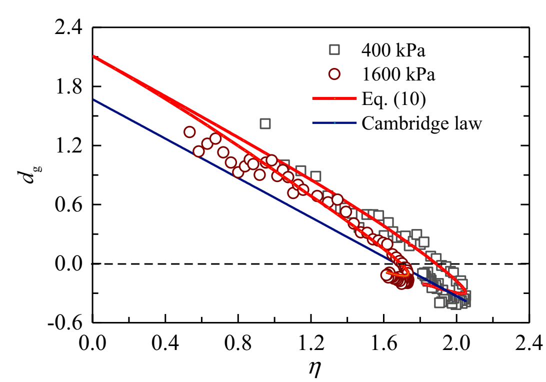

Fig. 9 Dilatancy behaviors of MRM

(10)] can well predict the observed characteristics of stress dilatancy.

It is worth mentioned that the mathematical form of Eq. (10) is so simple that the plastic potential function can be derived. Then, the fractional non orthogonal flow rule can be used to build fractional order constitutive model [31, 32]. The fractional non orthogonal flow rule means that loading direction can be derived according to the plastic potential function or plastic flow direction can be derived based on the yield function, and the angle between plastic flow direction and loading direction is determined by the order of the fractional derivative.

5 Verification

In order to examine the applicability of Eq. (10), the laboratory experimental results of drained triaxial shearing on TRM [33] and YXR [34] are arranged and the test data between $\frac{dE_b}{pd\varepsilon_s}$ and $M\Big/\sqrt{M_f}$ are fitted by Eq. (9) (Fig. 10). Figure 10 indicates that Eq. (9) proposed in this paper can well express the relationship between $\frac{dE_b}{pd\varepsilon_s}$ and $M\Big/\sqrt{M_f}$.

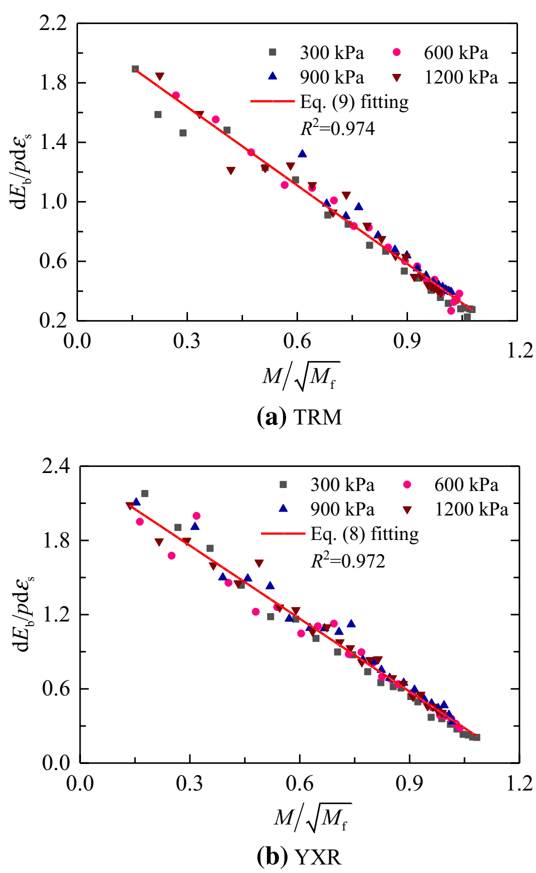

Fig. 10 Relationship between $\frac{dE_b}{pd\varepsilon_s}$ and $M\Big/\sqrt{M_f}$

Then, the comparison between predictions of Eq. (10) and the experimental data is shown in Fig. 11. As seen in Fig. 11, it is evident that Eq. (10) predicts the stress dilatancy relationship with acceptable accuracy.

6 Discussion of dilatancy equation parameters

λ can be determined according to $\lambda = 12.7/\varepsilon_{1c}$, but this way lacks practicality because generally CGS tested cannot reach the critical state. That is, ε_{1c} cannot be determined according to the triaxial test. The value of λ affects the calculation value of particle breakage energy. It is apparent from Eq. (3) that there is a negative correlation between λ and E_b and unreasonable value of λ can make the calculated particle breakage energy violate the thermodynamic, thus the value of λ needs to satisfy the thermodynamic law. Given that the reasonable calculation of particle breakage energy is only the carrier to investigate the stress dilatancy relationship of CGS, the focus of this paper is not the value of particle breakage energy but developing a simple and practical stress dilatancy relationship for CGS. Therefore, if the value of λ has no influence on the prediction results of Eq. (10) or this

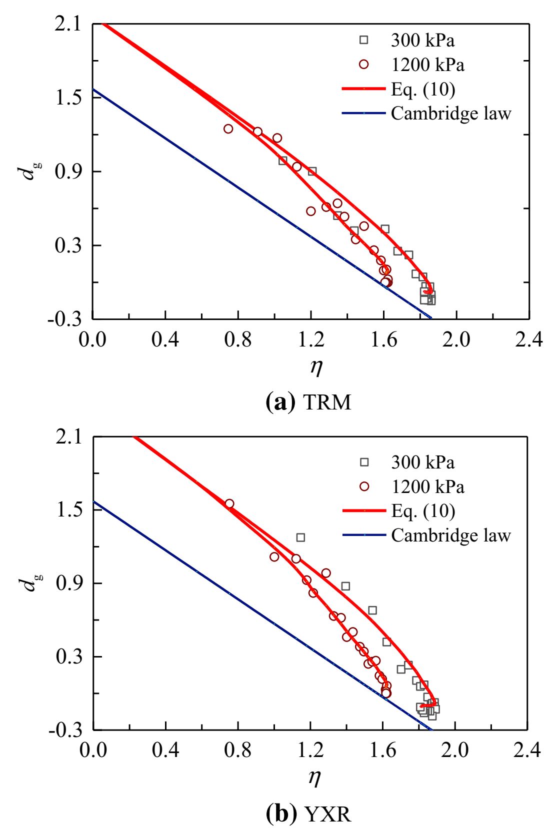

Fig. 11 The dilatancy behaviors of coarse-grained soils

influence is so little that it can be ignored, it will be enough that the value of λ satisfies the thermodynamic law.

Noting that the prediction efficiency of Eq. (10) is dependent of the fitting effect of $\frac{dE_b}{pd\varepsilon_s}$ and $M\Big/\sqrt{M_f}$ by Eq. (9). Figure 11 gives the calculated $\frac{dE_b}{pd\varepsilon_s}$ values and $M\Big/\sqrt{M_f}$ values corresponding to different values of λ. It can be seen from Figs. 8 and 12 that the value of λ has no impact on the fitting effect of $\frac{dE_b}{pd\varepsilon_s}$ and $M\Big/\sqrt{M_f}$ by Eq. (9). That is to say, the prediction efficiency of Eq. (10) is independent of λ. In general, the value of ε_{1c} is less than 40% for CGS. Thus taking ε_{1c} as 40% can satisfy the thermodynamic law, which is the reason for taking 40% as the value of ε_{1c} before.

In the proposed dilatancy equation incorporating four parameters, λ can be regarded as a constant. M_c is only related to the confining pressure, which can be obtained according to M_f. A and B are obtained by Eq. (9) fitting values of $\frac{dE_b}{pd\varepsilon_s}$ and $M\Big/\sqrt{M_f}$ of different confining pressures. Thus, A and B have no correlation with the confining pressure. To show the correlation between A and B and void ratio clearly, the triaxial compression test data of coarse-grained soils with different initial dry densities [23, 27] are arranged. Figure 13 shows the computed $\frac{dE_b}{pd\varepsilon_s}$ values and $M\Big/\sqrt{M_f}$ values. It is clear from Fig. 13 that excellent agreement is found between the computed $\frac{dE_b}{pd\varepsilon_s}$ values and $M\Big/\sqrt{M_f}$ values with different relative densities and the relationship between computed $\frac{dE_b}{pd\varepsilon_s}$ values and $M\Big/\sqrt{M_f}$ values can be fitted well by Eq. (9). That is, A and B can be regarded as irrelevant to void ratio.

7 Conclusions

Particle breakage can cause a shift in the stress dilatancy relationship of coarse-grained soils, and particle breakage energy can be used as a bridge to reflect the internal relationship between particle breakage and dilatancy behaviors. However, how to calculate particle breakage energy has yet to be satisfactorily addressed. To solve the dilemma, the reasonable calculation of particle breakage energy and the dilatancy relationship incorporating particle breakage energy

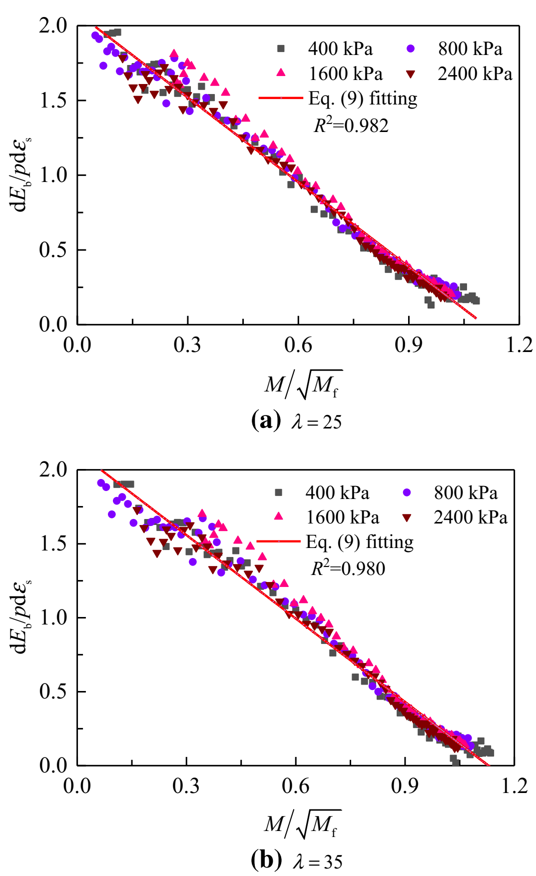

Fig. 12 Relationship between $\frac{dE_b}{pd\varepsilon_s}$ and $M\Big/\sqrt{M_f}$

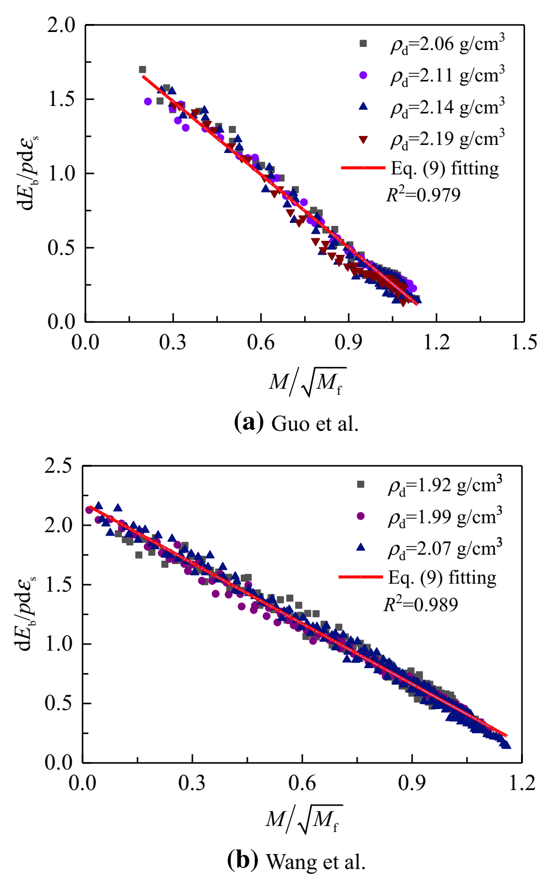

Fig. 13 Relationship between $\frac{dE_b}{pd\varepsilon_s}$ and $M\Big/\sqrt{M_f}$ with different initial dry densities

were investigated in this paper. The main conclusions are summarized as follows:

1. A energy balance equation for CGS was obtained by adding particle breakage into the Cambridge energy balance equation. Then the friction coefficient of this energy balance equation was modified based on the change law of particle breakage so that the reasonable calculation of particle breakage energy was realized, which satisfied the thermodynamic law.
2. The linear equation can describe the relationship between $\frac{dE_b}{pd\varepsilon_s}$ and $M\Big/\sqrt{M_f}$ with acceptable accuracy. Then a dilatancy equation considering particle breakage was developed by substituting this linear relationship into the energy balance equation, and this proposed dilatancy equation was able to simulate dilatancy behaviors of CGS well.
3. The proposed dilatancy equation incorporates four parameters, λ can be regarded as a constant, M_c is only related to the confining pressure, and A and B are independent of void ratio and the confining pressure, which can be regarded as the advantage of this proposed dilatancy equation.
4. The dilatancy equation proposed in this paper has a simple mathematical form, and the plastic potential function can be derived from this dilatancy equation. In the further study, with this derived plastic potential function, fractional non orthogonal flow rule can be used to build the fractional order constitutive model considering particle breakage.

Acknowledgements The authors gratefully acknowledge the financial support from National Key R&D Program of China (2018YFC1508505), and Yalong River Joint Fund of Natural Science Foundation of China—Yalong River Basin Hydropower Development Co., Ltd. (U1865104).

Data availability All data, models, and code generated or used during the study appear in the submitted article.

Declarations

Conflict of interest The authors declare that they have no conflict of interest.

References

1. Costa, L.M., Alonso, E.E.: Predicting the behavior of an earth and rockfill dam under construction. J. Geotech. Geoenviron. Eng. **135**(7), 851–862 (2009)
2. Xiao, Y., Liu, H.L., Ding, X.M., Chen, Y.M., Jiang, J.S., Zhang, W.G.: Influence of particle breakage on critical state line of rockfill material. Int. J. Geomech. **16**(1), 04015031 (2016)
3. Xu, M., Song, E.X., Chen, J.F.: A large triaxial investigation of the stress-path-dependent behavior of compacted rockfill. Acta Geotech. **7**(3), 167–175 (2012)
4. Nader, F., Silvani, C., Djeran-Maigre, I.: Grain breakage under uniaxial compression using a three-dimensional discrete element method. Granul. Matter **19**(3), 53–68 (2017)
5. Raisianzadeh, J., Mohammadi, S., Mirghasemi, A.A.: Micromechanical study of particle breakage in 2D angular rockfill media using combined DEM and XFEM. Granul. Matter **21**(3), 1–27 (2019)
6. Salim, W., Indraratna, B.: A new elastoplastic constitutive model for coarse granular aggregates incorporating particle breakage. Can. Geotech. J. **41**(4), 657–671 (2004)
7. Alonso, E.E., Tapias, M., Gili, J.: Scale effects in rockfill behaviour. Geotech. Lett. **2**(3), 155–160 (2012)
8. Indraratna, B., Salim, W.: Modeling of particle breakage of coarse aggregates incorporating strength and dilatancy. ICE Proc. Geotech. Eng. **155**(4), 243–252 (2002)
9. Chavez, C., Alonso, E.E.: A constitutive model for crushed granular aggregates which includes suction effects. Soils Found. **43**(4), 215–227 (2003)
10. Nimbalka, S., Indraratna, B., Dash, S.K., Christie, D.: Improved performance of railway ballast under impact loads using shock mats. J. Geotech. Geoenviron. Eng. **138**(3), 281–294 (2012)
11. Xiao, Y., Liu, H.L., Chen, Y.M.: State-dependent constitutive model for rockfill materials. Int. J. Geomech. **15**(5), 04014075 (2014)
12. Guo, W.L., Huang, Y.H., Andy, F., Wu, Y.L.: Mathematical model revealing the evolution of particle breakage and particle-size distribution for rockfill during triaxial shearing. Eur. J. Environ. Civ. Eng. **25**, 893–908 (2019)
13. Bandini, V., Coop, M.R.: The influence of particle breakage on the location of the critical state line of sands. Soils Found. **51**(4), 591–600 (2011)
14. Alaei, E., Mahboubi, A.: A discrete model for simulating shear strength and deformation behavior of rockfill material, considering the particle breakage phenomenon. Granular Matter **14**(6), 707–717 (2012)
15. Ueng, T.S., Chen, T.J.: Energy aspects of particle breakage in drained shear of sands. Geotechnique **50**(1), 65–72 (2000)
16. Szypcio, Z.: The influence of particle breakage on stress-dilatancy relationship for granular soils. In: E3S Web of Conferences, vol. 92, p. 09004 (2019)
17. Rowe, P.W.: The stress-dilatancy relation for the static equilibrium of an assembly of particles in contact. Proc. R. Soc. A Math. Phys. Eng. Sci. **269**(1339), 500–527 (1962)
18. Roscoe, K.H., Schofield, A.N., Thurairajah, A.: Yield of clays in state wetter than critical. Geotechnique **13**(3), 211–240 (1963)
19. Jia, Y.F., Chi, S.C., Yang, J., Lin, G.: Measurement of breakage energy of coarse granular aggregates. Rock Soil Mech. **30**(7), 1960–1966 (2009)
20. Mi, Z.K., Li, G.Y., Chen, S.S.: Constitutive model for coarse granular materials based on breakage energy. Chin. J. Geotech. Eng. **34**(10), 1801–1811 (2012)
21. Guo, W.L., Zhu, J.G.: Particle breakage energy and stress dilatancy in drained shear of rockfills. Geotech. Lett. **7**(4), 1–20 (2017)
22. ASTM D2487: Standard practice for classification of soils for engineering purposes (unified soil classification system). West Conshohocken (2017)
23. Wang, L., Zhu, J.G., Zhang, Z.L., Zheng, H.F.: Effects of dry density on shear behavior and particle breakage forslate rockfill material. Bull. Eng. Geol. Environ. **80**(2), 1181–1192 (2019)
24. Guo, W.L., Cai, Z.Y., Wu, Y.L., Huang, Y.H.: Study on the particle breakage energy and dilatancy of coarse-grained soils. Rock Soil Mech. **40**(12), 1–9 (2019)

25. Wu, Y.L., Huangfu, Z.H., Guo, W.L., Zhang, Z.S.: Influence of particle breakage on critical state of coarse-grained soils. Chin. J. Geotech. Eng. **41**(2), 25–28 (2019)
26. Ning, F.W., Liu, J.M., Kong, X.J., Zou, D.G.: Critical state and grading evolution of rockfill material under different triaxial compression tests. Int. J. Geomech. **20**(2), 04019154 (2020)
27. Guo, W.L., Cai, Z.Y., Wu, Y.L., Geng, Z.Z.: Estimations of three characteristic stress ratios for rockfill material considering particle breakage. Acta Mech. Solida Sin. **32**(2), 215–229 (2019)
28. Jia, Y.F., Xu, B., Chi, S.C., Xiang, B., Zhou, Y.: Research on the particle breakage of rockfill materials during triaxial tests. Int. J. Geomech. **17**(10), 04017085 (2017)
29. Wang, F., Zhang, J.Q.: Study of breakage behavior of original rockfill materials considering size effect on particle strength. Rock Soil Mech. **41**(1), 87–94 (2020)
30. Wu, E.L., Zhu, J.G., Huang, W., Liu, Z.: Evolution law of particle breakage of coarse-grained soil during triaxial shearing. Chin. J. Geotech. Eng. **42**(12), 2330–2335 (2020)
31. Sun, Y.F., Xiao, Y.: Fractional order plasticity model for granular soils subjected to monotonic triaxial compression. Int. J. Solids Struct. **118–119**(1), 224–234 (2017)
32. Sun, Y.F., Shen, Y.: Constitutive model of granular soils using fractional-order plastic-flow rule. Int. J. Geomech. **17**(8), 04017025 (2017)
33. Xiao, Y., Liu, H.L.: Elastoplastic constitutive model for rockfill materials considering particle breakage. Int. J. Geomech. **17**(1), 044016041 (2017)
34. Sun, H.Z., Huang, M.S.: A constitutive model for coarse granular material incorporating both strain work-softening and dilatancy. J. Tongji Univ. (Nat. Sci.). **37**(6), 727–732 (2009)